Coordination Chemistry Reviews, 97 (1990) 105–117
Elsevier Science Publishers B.V., Amsterdam — Printed in The Netherlands

MULTIELECTRON PHOTOCHEMISTRY OF QUADRUPLY BONDED METAL-METAL COMPLEXES

COLLEEN M. PARTIGIANONI, I-JY CHANG, and DANIEL G. NOCERA

Department of Chemistry, Michigan State University, East Lansing, MI 48824

ABSTRACT

The structural, electronic, and oxidation-reduction properties of multiply bonded metal-metal ($\mathrm{M}\overset{n}{\text{—}}\mathrm{M}$) dimers presage a rich excited state chemistry for these complexes. Our work has emphasized photochemical pathways that utilize $\mathrm{M}\overset{4}{\text{—}}\mathrm{M}$ dimers to promote overall multielectron transformations. Multielectron photochemistry can only be achieved by correctly manipulating the molecular and electronic structures of these dimers such that one-electron pathways are circumvented. We now present a summary of the strategy used for the rational design of $\mathrm{M}\overset{4}{\text{—}}\mathrm{M}$ multielectron photochemical schemes.

INTRODUCTION

Oxidation-reduction transformations of transition metal complexes in electronic excited states have been a longstanding thematic focus of inorganic photochemistry. Numerous investigations during the past two decades have proven single electron transfer to be an ubiquitous redox pathway of electronically excited transition metal complexes [1-4]. Because many desirable oxidation-reduction processes such as small molecule activation involve the transfer of two or more electrons, recent efforts have been extended to include the utilization of electronically excited molecules to promote multielectron transformations. Successful multielectron photochemical schemes to date have relied on coupling one-electron excited state chemistry via a relay catalyst [5] or by photochemically generating reactive intermediates that undergo subsequent oxidation or reduction [6-8]. One approach that we have explored in designing novel multielectron schemes relies on exploiting the complementary redox function of two metals of electron rich metal-metal bonds beginning with quadruply bonded ($\mathrm{M}\overset{4}{\text{—}}\mathrm{M}$) dimers. The structural, electronic, and redox properties of these dimers suggest them to be promising multielectron photoreagents. The lowest energy excited states of these complexes are long-lived and metal localized [9,10]. Moreover, the $\mathrm{M}\overset{4}{\text{—}}\mathrm{M}$ core is a two-electron source or sink in oxidation-reduction reactions and coordinatively unsaturated [11,12]. The ability to coordinate substrate molecules to a long-lived, electronically excited metal core that exhibits multielectron redox activity suggested to us the possibility of a rich multielectron photochemistry for $\mathrm{M}\overset{4}{\text{—}}\mathrm{M}$ complexes. Described herein are studies aimed at providing guidelines for the systematic development of a framework in which to explore novel multielectron photoreactions of $\mathrm{M}\overset{4}{\text{—}}\mathrm{M}$ dimers.

0010-8545/90/$04.55

PHOTOCHEMISTRY OF $\mathrm{M}\overset{4}{-}\mathrm{M}$ PHOSPHATES IN ACIDIC SOLUTIONS

Conversion of a $\mathrm{M}\overset{n}{-}\mathrm{M}$ dimer with a metal bond order of 4 to a species of bond order 3 constitutes a two-electron process and conceptually represents the simplest multielectron transformation available to a $\mathrm{M}\overset{4}{-}\mathrm{M}$ system. Accordingly initial experiments were directed towards exploring the two-electron reduction of a proton by electronically excited $\mathrm{M}\overset{4}{-}\mathrm{M}$ dimers to yield a hydride which could then subsequently be trapped by a proton to give hydrogen according to the following reaction scheme:

$$\mathrm{M}\overset{4}{-}\mathrm{M}^{n-} \xrightarrow{h\nu} \mathrm{M}\overset{4}{-}\mathrm{M}^{n-*} \qquad (1)$$

$$\mathrm{M}\overset{4}{-}\mathrm{M}^{n-*} + \mathrm{H}^+ \longrightarrow \underset{\mathrm{H}}{\mathrm{M}\overset{3}{-}\mathrm{M}}^{(n-1)-} \qquad (2)$$

$$\underset{\mathrm{H}}{\mathrm{M}\overset{3}{-}\mathrm{M}}^{(n-1)-} + \mathrm{H}^+ \longrightarrow \mathrm{M}\overset{3}{-}\mathrm{M}^{(n-2)-} + \mathrm{H}_2 \qquad (3)$$

Despite the simplicity of this scheme, previous studies of $\mathrm{M}\overset{4}{-}\mathrm{M}$ dimers indicate two-electron processes to be exceptional reaction pathways and $\mathrm{M}\overset{4}{-}\mathrm{M}$ excited state chemistry has been limited to the one-electron oxidation of the metal-metal bond. For instance, under relatively strong oxidizing conditions, irradiation ($\lambda \leq 254$ nm) of $Mo_2(SO_4)^{4-}$ in H_2SO_4 yields the one-electron mixed-valence product $Mo_2(SO_4)_4^{3-}$ [13]. The above scheme is predicated on a quadruple↔triple bond interconversion. Presumably, the chemical instability of the triply-bonded sulfate complex precludes multielectron photochemistry. To this end, the discovery of the triple bond dimer $Mo_2(HPO_4)_4^{2-}$ by Avi Bino and Al Cotton [14] prompted our synthesis of the analogous quadruply bonded species $Mo_2(HPO_4)_4^{4-}$ [15]. Whereas $Mo_2(HPO_4)_4^{4-}$ thermally reacts in 2 M H_3PO_4 to produce the mixed-valence species $Mo_2(HPO_4)_4^{3-}$ and H_2 over a period of days, ultraviolet irradiation ($\lambda >$ 335 nm) of phosphoric acid solutions of the dimer leads to the prompt production of the two-electron oxidized dimer $Mo_2(HPO_4)_4^{2-}$ and H_2 [15]. The appearance of the characteristic $\delta^2 \rightarrow \delta\delta^*$ transition of $Mo_2(HPO_4)_4^{3-}$ in the infrared spectral region and our observation of the production of the triple bonded dimer $Mo_2(HPO_4)_4^{2-}$ upon irradiation of the mixed-valence species suggests that the over multielectron photooxidation of $Mo_2(HPO_4)_4^{4-}$ proceeds by the sequential reaction sequence.

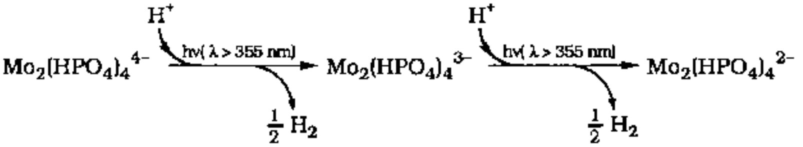

$$Mo_2(HPO_4)_4^{4-} \xrightarrow[-\frac{1}{2}H_2]{H^+,\ h\nu(\lambda > 355\ nm)} Mo_2(HPO_4)_4^{3-} \xrightarrow[-\frac{1}{2}H_2]{H^+,\ h\nu(\lambda > 355\ nm)} Mo_2(HPO_4)_4^{2-} \qquad (4)$$

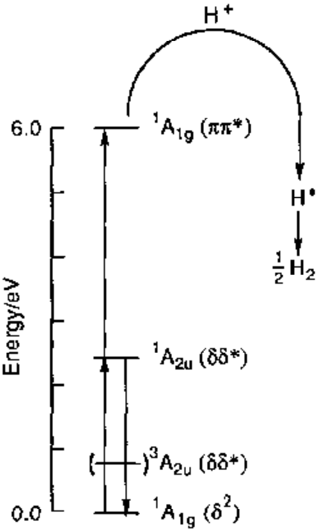

Figure 1. State diagram for the reaction of $M\overset{n}{—}M$ in acidic solution to produce H_2 and $M\overset{n-1/2}{—}M$.

An action spectrum reveals that the quantum yield for reaction 4 asymptotically approaches a maximum value of 0.05 at wavelengths less than 300 nm. This wavelength region of maximum photochemical activity is coincident with the energies of the allowed $\pi \rightarrow \pi\pi^*$ transition of the Mo_2 phosphates, thereby suggesting that the primary photochemical step involves direct production of hydrogen atoms via the $\pi\pi^*$ excited state. Photochemical trapping experiments support this contention. Ultraviolet irradiation of $Mo_2(HPO_4)_4{}^{n-}$ (n = 3, 4) in N_2O saturated 2 M H_3PO_4 solutions yields the one-electron photooxidized Mo_2 phosphato complex and N_2. Nitrogen, which is generated at the expense of hydrogen, is the product expected from the reaction of hydrogen atoms with N_2O [16].

The proposed reaction sequence for the Mo_2 phosphato complexes is summarized in Figure 1. Excitation to produce the powerfully reducing $\pi\pi^*$ excited state of $Mo_2(HPO_4)_4{}^{n-}$ (n = 3, 4) results in direct reduction of protons to H atoms. Annihilation of two hydrogen atoms or subsequent oxidation of the Mo_2 starting complex by a hydrogen atom to yield H^- followed by facile proton trapping will result in hydrogen production. Our observation that photooxidation is confined to one-electron primary photoprocesses of the high energy $\pi\pi^*$ excited state conforms well with the general reactivity pattern emerging for $M\overset{4}{—}M$ dimers in acidic solution. Namely, reaction from the lowest energy excited states (*e.g.* $^1\delta\delta^*$) is circumvented in acidic solutions. For instance, the production of hydrogen and $Mo_2(SO_4)^{3-}$ upon $Mo_2(SO_4)^{4-}$ photolysis also occurs with frequencies coincident with the $\pi\pi^*$ excited state. That the mixed-valence sulfato dimer does not further react, as is the case for the Mo_2 phosphato system, simply reflects the increased susceptibility of the Mo_2 core towards oxidation when ligated by phosphate as opposed to sulfate.

In regard to the design of multielectron schemes, an important issue is why isn't the potential multielectron reactivity of the lowest energy excited states of these dimers accessed in acidic solution? Recent studies in our laboratories have established that the $^1\delta\delta^*$ excited states of $M\overset{4}{—}M$ dimers are especially susceptible to proton quenching, and similar to the insidious energy wasting back-electron transfer problem, provides a facile decay route to ground state. For example, the luminescence of the $Re_2Cl_8^{2-}$ ion ($\lambda_{em,max}$ = 760 nm, τ_o = 150 ns) in CH_3CN solutions is markedly attenuated upon the addition of nonaqueous acids such as trifluoromethanesulfonic acid. Stern-Volmer plots of the luminescence intensity *vs.* acid concentration are linear and yield a rate constant for quenching of 1.6×10^9 M^{-1} s^{-1}. These results suggest that if the potential multielectron chemistry of the lower energy excited states is to be exploited and the one-electron reactions of higher energy excited states circumvented, then proton quenching of the $M \overset{4}{-} M$ luminescence and energy wasting back reaction must be avoided.

PHOTOCHEMISTRY OF $M \overset{4}{-} M$ PHOSPHATES IN NONAQUEOUS SOLUTION

The absence of any appreciable lifetime for $M \overset{4}{-} M$ complexes in acidic solution prompted us to undertake studies of Mo_2 phosphates in aprotic solution. To this end, the Mo_2 dialkyl and diaryl phosphates $Mo_2[O_2P(OR)_2]_4$ (R = C_6H_5, C_2H_5, C_4H_9), which exhibit good solubility in nonaqueous solutions, were prepared and structurally and electronically characterized [17]. The electronic absorption spectrum of $Mo_2[O_2P(OC_6H_5)_2]_4$ is dominated by the prominent $^1(\delta^2 \rightarrow \delta\delta^*)$ band and is virtually identical to that of $Mo_2(HPO_4)_4^{4-}$ ($\lambda_{abs,max}$ (ε) = 515 nm (156 M^{-1} cm^{-1}) and 516 nm (196 M^{-1} cm^{-1}) for $Mo_2[O_2P(OC_6H_5)_2]_4$ and $Mo_2(HPO_4)_4^{4-}$, respectively). However, in contrast to $Mo_2(HPO_4)_4^{4-}$, solids and solutions of Mo_2(II,II) diphenyl phosphate exhibit luminescence ($\lambda_{em,max}$ = 560 nm) upon excitation into the $^1(\delta^2 \rightarrow \delta\delta^*)$ absorption band. Because the emission quantum yield for this complex is low (ϕ_e = 10^{-4}), the lifetime of the $^1\delta\delta^*$ excited state is most easily measured by transient absorption spectroscopy. The decay of the $^1\delta\delta^*$ excited state is monoexponential and the measured lifetime of 68 ns (Figure 2) is sufficiently long-lived to permit the bimolecular reaction of this singlet excited state with substrate molecules.

Whereas halocarbon solutions are indefinitely stable in the absence of light, reaction of these solutions is immediate upon visible irradiation. For instance, photolysis (λ_{exc} > 530 nm) of Mo_2(II,II) diphenyl phosphate in solutions of 1,2-dichloroethane (DCE) causes the $^1(\delta^2 \rightarrow \delta\delta^*)$ absorption band to monotonically decrease in intensity with a concomitant increase in absorption in the near-infrared spectral region. The appearance of this vibrationally-structured absorption in the near-infrared ($\lambda_{abs,max}$ (ε) = 1494 nm (362 M^{-1} cm^{-1})) is consistent with the production of the mixed-valence Mo_2(II,III) diphenyl phosphate dimer. Indeed, the formation of $Mo_2[O_2P(OC_6H_5)_2]_4Cl$ as the photoproduct has been verified by its independent preparation and characterization. The maximum quantum yield of ϕ_p = 0.040 ± 0.004 observed for irradiation wavelengths in the 490-540 nm spectral range is consistent with the photoreaction originating directly from the $^1\delta\delta^*$ excited

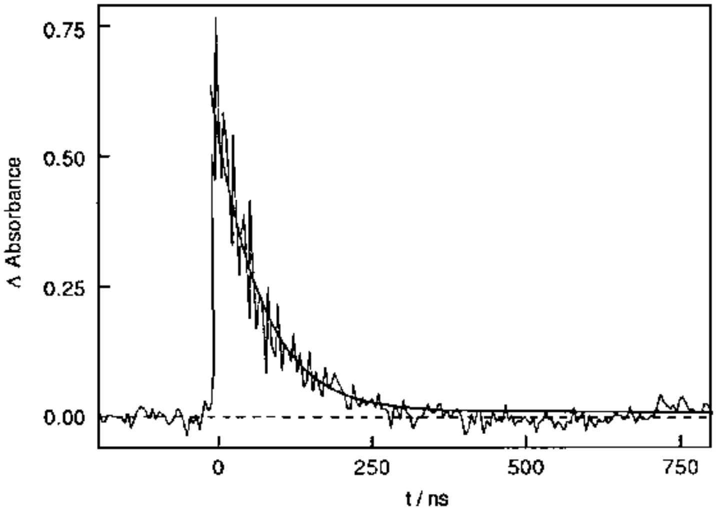

Figure 2. Transient absorption kinetics of $Mo_2[O_2P(OC_6H_5)_2]_4$ in THF at room temperature. The monitoring wavelength was 460 nm and the decay curve was recorded 250 ps after excitation with a 532-nm Nd:YAG laser pulse (FWHM = 25 ps).

state. Toepler pumping of the photochemical reaction mixture gave 0.51 ± 0.03 equivalents of ethylene, as determined by GC/MS analysis. This production of 0.5 equivalents of ethylene in conjunction with the quantitative formation of the mixed-valence dimer has lead us to propose [17] the following photochemical reaction mechanism

$$Mo_2[O_2P(OC_6H_5)_2]_4 \xrightarrow{h\nu} Mo_2[O_2P(OC_6H_5)_2]_4{}^* \qquad (5)$$

$$Mo_2[O_2P(OC_6H_5)_2]_4 + ClCH_2CH_2Cl \longrightarrow Mo_2[O_2P(OC_6H_5)_2]_4Cl + {}^\bullet CH_2CH_2Cl \qquad (6)$$

$$Mo_2[O_2P(OC_6H_5)_2]_4 + {}^\bullet CH_2CH_2Cl \longrightarrow Mo_2[O_2P(OC_6H_5)_2]_4Cl + CH_2CH_2 \qquad (7)$$

An estimated $E_{0,0}(Mo_2[O_2P(OC_6H_5)_2]_4{}^*) = 2.3$ eV and a measured $E_{1/2}[Mo_2(II,II)/Mo_2(II,III)] = -0.1$ V *vs.* SCE establishes that the electronically excited $Mo_2[O_2P(OC_6H_5)_2]_4$ is sufficiently energetic to directly react with DCE to yield ${}^\bullet CH_2CH_2Cl$ and $Mo_2[O_2P(OC_6H_5)_2]_4Cl$. Subsequent reaction of the radical with another equivalent of Mo_2(II,II) starting complex directly yields the observed photoproducts.

The Mo_2(II,II) diphenyl phosphate system is interesting from a design standpoint because the two-electron photochemistry of $M \overset{4}{—} M$ species has

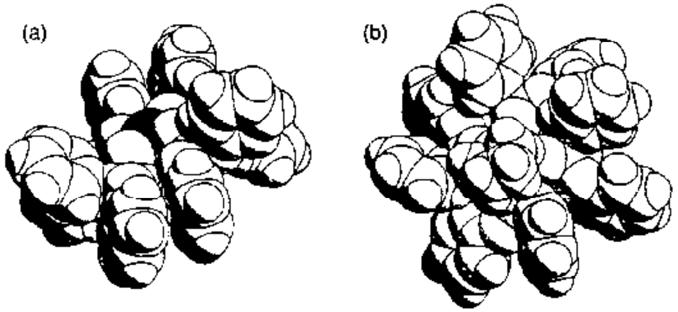

Figure 3. Computer generated space-filling models of (a) $Mo_2[O_2P(OC_6H_5)_2]_4$ and (b) $Mo_2[O_2P(OC_6H_5)_2]_4 \cdot 2THF$. The Mo center is denoted by the black ball.

been moved from the ultraviolet to the visible spectral region. Nevertheless, the overall multielectron process is achieved by coupling the redox function of independent metal cores. Insight into why the Mo_2(II,II) phosphate is confined to one-electron excited state reaction is provided by computer models generated from the atomic coordinates determined from the X-ray structural analysis of $Mo_2[O_2P(OC_6H_5)_2]_4$. Figure 3a shows the space-filling computer model of $Mo_2[O_2P(OC_6H_5)_2]_4$ situated just off-axis of its metal-metal bond. Inspection of the model reveals that the δ and δ^* orbitals, which are potentially important to multielectron reactivity, are totally shielded by the diphenyl phosphate ligands. Alternatively, the metal-metal core is clearly visible to axially approaching substrates. Thus $Mo_2[O_2P(OC_6H_5)_2]_4$ photochemistry appears to be confined to attack by substrate at the axial coordination site of the metal-metal core. Quantum yield data support this analysis. Table 1 lists

TABLE 1

Quantum Yield Data for the Reaction of $Mo_2[O_2P(OC_6H_5)_2]_4$ and DCE in Various Nonaqueous Solvents

Solvent	[DCE] / M	ϕ_p[a]
DCE	13	0.040
Benzene	9	0.031
THF	9	0.014
CH3CN	9	0.001

[a] Determined by using a ferrioxalate actinometer.

the photochemical quantum yield, ϕ_p, for the reduction of DCE by $Mo_2[O_2P(OC_6H_5)_2]_4$ in a variety of solvents. The quantum yields decrease dramatically with the increasing ability of solvent to ligate the metal core in the axial coordination site. For the case of THF, the crystal structure of $Mo_2[O_2P(OC_6H_5)_2]_4 \cdot 2THF$ has been solved and as the model in Figure 3b shows, the ligating solvent molecules completely insulate the metal-metal core from substrate. Consequently, the photoreduction of DCE by $Mo_2[O_2P(OC_6H_5)_2]_4$ is severely impeded.

MULTIELECTRON PHOTOTRANSFORMATIONS OF $M\overset{4}{—}M$ DIMERS AT A DISCRETE BINUCLEAR METAL CORE

The structure/photoreactivity relationship established for the $Mo_2(II,II)$ phosphate system suggests that not only is the presence of long-lived lowest energy excited state a necessary condition for $M\overset{4}{—}M$ multielectron photochemistry, but substrates must access the metal core with the proper orientation such that the complementary redox function of both metals of an individual electronically excited core is exploited. Moreover, the lowest energy excited states of $M\overset{4}{—}M$ dimers ($\delta \rightarrow \delta^*$, $\delta \rightarrow \pi^*$, and $\pi \rightarrow \delta^*$) are highly localized between the metals of the binuclear core, and little electron density is present in the axial coordination sites. To this end, we became interested in $M\overset{4}{—}M$ dimers with less sterically confined metal cores thereby permitting equatorial approach of substrate. Not only can both metals be accessed by substrate, but the δ and π orbitals exhibit maximum directionality in the equatorial plane.

The steric congestion in the equatorial plane of the $M_2X_4(\overparen{PP})_2$ ($\overparen{PP}$ = bridging phosphine, X = halide) complexes is greatly reduced owing to the presence of the four halides. Our initial studies have been focused on the ditungsten complex $W_2Cl_4(dppm)_2$ (dppm = diphenylphosphinomethane) [18]. Although CH_3I solutions of $W_2Cl_4(dppm)_2$ are indefinitely stable at room temperature in the absence of light, excitation with $\lambda > 436$ nm results in the spectral changes shown in Figure 4. The decrease in the absorption maximum of the $\delta \rightarrow \delta^*$ transition is accompanied by the appearance of absorptions at 490 and 582 nm and a weak near-infrared transition at 1090 nm. Importantly, the intense near-infrared absorption in the 1400 - 1600 nm spectral region that is characteristic of mixed-valence $M\overset{3.5}{—}M$ dimers [19] is not observed. Consistent with the presence of the isosbestis points, a single product is quantitatively isolated. We have shown by elemental and spectroscopic analyses that the product corresponds to addition of CH_3I to the tungsten-tungsten bond to yield $W_2Cl_4(dppm)_2(CH_3)(I)$. The coordination geometry about the tungsten-tungsten bond has yet to be unequivocally established owing to our inability to obtain single crystals suitable for X-ray

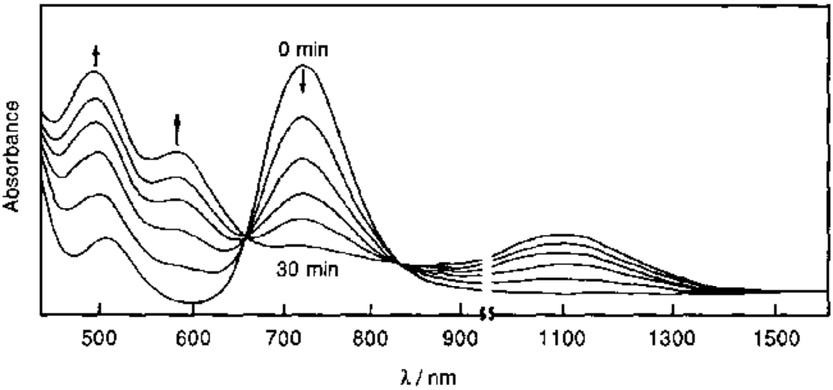

Figure 4. Spectral changes resulting from the photolysis of deoxygenated methyl iodide solutions of $W_2Cl_4(dppm)_2$.

structural analysis. However, the absorption profile of the final photolysis spectrum in Figure 4 displaying weak near-infrared and visible absorptions centered around 500 nm are characteristic of edge-sharing bioctahedral complexes in which the metal core is strapped by the bridging ligands in a trans configuration [20,21]. Information about the coordination position of the methyl group is provided by ^{13}C nmr spectra, which show a single resonance shifted 21 ppm upfield from TMS. This result suggests that the methyl group is in a terminal rather than a bridging position because the diamagnetic anisotropy of the metal-metal bond is expected to induce a downfield shift for ligands occupying bridging coordination sites [22].

The oxidative-addition product is formed with a quantum yield of 0.029. Interestingly, the spectral range for the maximum quantum yield is energetically coincident with excitation of the metal-localized $\delta\pi^*$ and $\pi\delta^*$ transitions. In accordance with these observations, time-resolved transient absorption studies of $M_2X_4P_4$ complexes have identified the presence of transients consistent with $\delta\pi^*$ and $\pi\delta^*$ parentages that possess lifetimes an order of magnitude greater than that observed for the $\delta\delta^*$ excited state [10].

The photochemistry of the $W_2Cl_4(dppm)_2$ is in marked contrast to the thermal oxidation chemistry of $M_2X_4(\overset{\frown}{PP})_2$ complexes which do not necessarily yield products corresponding to the direct addition of substrate to the metal-metal core. For example, the thermal reaction of $Mo_2Cl_4(dppm)_2$ with PhSSPh (Ph = phenyl) yields the edge-sharing bioctahedral $Mo_2Cl_4(dppm)_2(\mu\text{-}Cl)(\mu\text{-}SPh)$ [20]. We have found that this pentachloro product is characteristic of free radical reactions of $M_2X_4(\overset{\frown}{PP})_2$ complexes. Our most compelling evidence

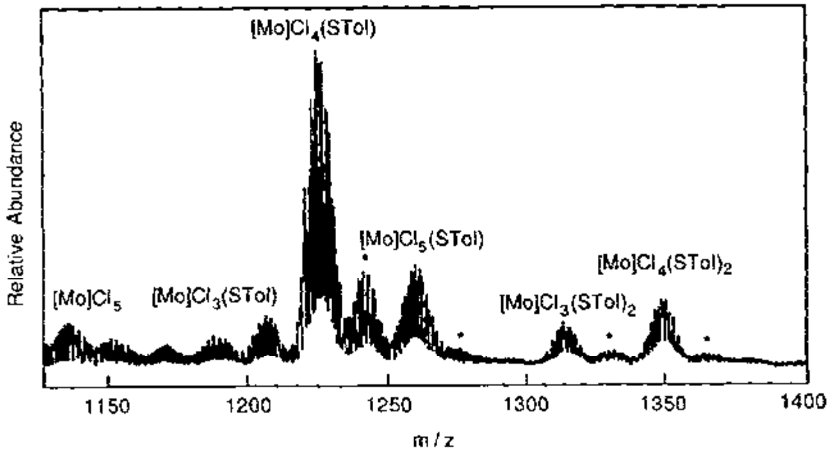

Figure 5. Fast atom bombardment mass spectrum of photolyzed (λ_{exc} > 436 nm) solutions of $Mo_2Cl_4(dppm)_2$ and tolyl disulfide. Selected peak assignments are shown above where [Mo] = $Mo_2(dppm)_2$. Each ion cluster is flanked by a solvent adduct peak, which is indicated by an asterisk.

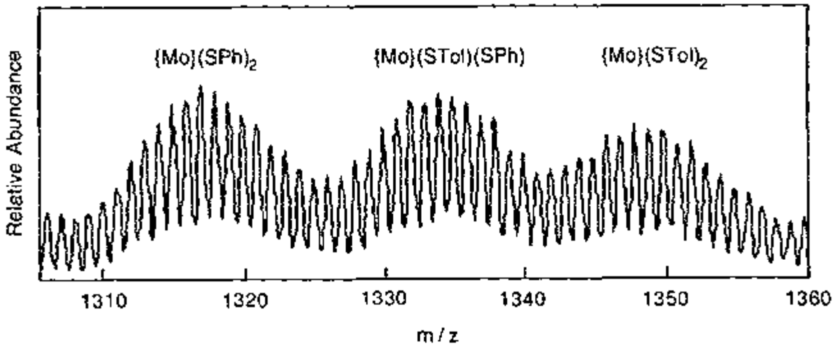

Figure 6. Molecular ion cluster region of the fast atom bombardment mass spectra of photolyzed (λ_{exc} > 436 nm) solutions of $Mo_2Cl_4(dppm)_2$ in the presence of phenyl/tolyl disulfide mixtures. {Mo} = $Mo_2Cl_4(dppm)_2$.

comes from investigations of the photochemistry of $Mo_2Cl_4(dppm)_2$ with disulfides. Figure 5 shows the FABMS of photolyzed (λ_{exc} > 436 nm) solutions of $Mo_2Cl_4(dppm)_2$ and tolyl disulfide (TolSSTol). A cluster centered at 1350 m/z corresponds to the parent molecular ion of $Mo_2Cl_4(dppm)_2(STol)_2$, with major fragments centered at 1315 and 1228 m/z corresponding to the loss of Cl and STol, respectively. In addition, a parent ion peak at 1264 m/z representing the pentachloro product $Mo_2Cl_5(dppm)_2(STol)$ is also observed. That the reaction proceeds by a free radical mechanism is substantiated by the irradiation of solutions containing equimolar mixtures of phenyl and tolyl disulfides. As Figure 6 shows, the molecular ion region reveals the presence of not only $Mo_2Cl_4(dppm)_2(STol)_2$ and $Mo_2Cl_4(dppm)_2(SPh)_2$, but the crossover product $Mo_2Cl_4(dppm)_2(STol)(SPh)$ as well. The presence of the crossover product strongly suggests the presence of free radical intermediates (solutions of $Mo_2Cl_4(dppm)_2(SPh)_2$ and $Mo_2Cl_4(dppm)_2(STol)_2$ show no evidence of exchange). Similarly thermal and photochemical reactions of $W_2Cl_4(dppm)_2$ in the presence of bulky iodides also yield the pentachloro product $W_2Cl_5(dppm)_2I$ and the diiodo species $W_2Cl_4(dppm)_2I_2$. We can account for the formation of the pentachloro and $M_2Cl_4(dppm)_2X_2$ (X = I, STol) products by invoking a radical mechanism wherein the $M_2Cl_4(dppm)_2$ complex reacts with XY (Y = alkyl, STol) to produce the mixed-valence $M_2(dppm)_2Cl_4(X)$ which disproportionates by either chlorine or X atom transfer to yield $M_2Cl_5(dppm)_2X$ and $M_2Cl_4(dppm)_2X_2$ as follows,

$$M_2Cl_4(dppm)_2 \xrightarrow{h\nu} M_2Cl_4(dppm)_2{}^{*} \tag{8}$$

$$M_2Cl_4(dppm)_2{}^{*} + XY \longrightarrow M_2Cl_4(dppm)_2X + {\bullet}Y \tag{9}$$

$$2M_2Cl_4(dppm)_2X \left\{ \begin{array}{ll} \rightarrow M_2Cl_5(dppm)_2X + M_2Cl_3(dppm)_2X & (10) \\ \rightarrow M_2Cl_4(dppm)_2X_2 + M_2Cl_4(dppm)_2 & (11) \end{array} \right.$$

Preliminary electrochemical experiments support the disproportionation reaction of $M_2Cl_5(dppm)_2X$ as described by eqs 10 and 11. A similar disproportionation mechanism involving halogen atom transfer between mixed-valence intermediates for the photochemical reaction of diplatinum pyrophosphite with aryl halides has been previously proposed [23].

The important observations in regard to the $W_2Cl_4(dppm)_2$ photoreaction with methyl iodide are (i) the products $W_2Cl_5(dppm)_2I$ and $W_2Cl_4(dppm)_2I_2$ that would be generated by the free radical mechanism described by reactions 8 - 11 are not observed and (ii) ethane, which would result from the combination of methyl radicals, is not detected. These observations in conjunction with the production of $W_2Cl_4(dppm)_2(CH_3)(I)$ as the sole photoproduct establish that the two-electron photoreduction of substrate has occurred at a discrete ditungsten core.

An issue of significant interest is the nature of the discrete multielectron transformation. The weak coupling between the d_{xy} orbitals of individual metals in the $M\overset{4}{-}M$ core is manifested in the low energy excited states involving the δ orbitals acquiring considerable ionic character. Accordingly, valence structures of the type shown by **1** could be important in promoting concerted addition of CH_3I to the metal core. Alternatively, the photochemical oxidative reaction may proceed by sequential electron transfer within a solvent cage. In this case, the incipient radical produced from substrate attack in the equatorial plane will be immediately trapped by the neighboring metal center as depicted by intermediate **2**. Due to the distinct absorption profiles of the

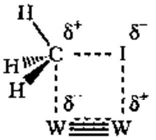

1

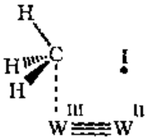

2

$\mathrm{M}\overset{n}{-}\mathrm{M}$ species (n = 3, 3.5, and 4), picosecond transient absorption spectroscopy may be employed to distinguish between a concerted pathway to yield intermediates such as **1** and a pathway involving electron transfer within a solvent cage to produce **2**. These studies are currently underway.

SUMMARY

Thus structural and electronic properties of $\mathrm{M}\overset{4}{-}\mathrm{M}$ dimers can be tailored to promote multielectron phototransformations by coupling the one-electron redox chemistry of individual metal cores in sequential steps or by exploiting the two-electron activity of a discrete metal core in an effective single step. In regard to the design of photochemical schemes relying on the latter pathway, reactivity from high energy excited states must be avoided. As illustrated with the Mo_2 phosphate system, the substantial kinetic barriers of many one-electron reactions such as the reduction of protons to hydrogen atoms are easily surmounted from the high energy excited states of $\mathrm{M}\overset{4}{-}\mathrm{M}$ dimers. Although fewer one-electron reaction pathways can be accessed from lower energy excited states, single electron transfer remains as a viable reaction pathway of $\mathrm{M}\overset{4}{-}\mathrm{M}$ complexes. We believe that the issue of one- or two-electron reactivity from low energy excited states is influenced in part by the orientation of substrate with respect to the metal-metal core. In the case of the Mo_2 diaryl phosphates, the photoactivated metal core is insulated by its ligating coordination sphere and substrate attack is confined to the axial site of the metal core. The overall multielectron chemistry is initiated by single electron transfer from the axially approached metal. By reducing the steric congestion in the equatorial plane of the $\mathrm{M}\overset{4}{-}\mathrm{M}$ core the complementary redox function of both metal centers can be accessed by substrate. Two-electron reduction of CH_3I proceeds smoothly at the electronically excited ditungsten core of $W_2Cl_4(dppm)_2$. By increasing the steric bulk of the substrate (*i.e.* isopropyl iodide or aryl disulfides), the reaction is channelled along one-electron free radical pathways. Of course, it is unlikely that steric factors alone determine the course of oxidation-reduction reactions of the low energy excited states of $M\overset{4}{-}M$ dimers. The nature of the substrate, the electronically excited complex, and environment will all play importamt contributing roles to the observed photoredox chemistry of these dimers. As these factors continue to be more clearly defined, we hope that principles for the facile design of a variety of multielectron photochemical schemes will begin to emerge.

ACKNOWLEDGEMENT

This work was supported by grants from the National Science Foundation, AMAX Foundation, Research Corporation, and a Henry and Camille Dreyfus Grant for Newly Appointed Young Faculty in Chemistry. DGN also gratefully acknowledges the support provided by a Presidential Young Investigator Award, administered by the National Science Foundation. We express our gratitude to Dr. Jay Winkler for providing access to the picosecond laser facilities at Brookhaven National Laboratory.

REFERENCES

1. M. A. Fox, M. Chanon, (Eds.), Photoinduced Electron Transfer, Elsevier, Amsterdam, 1988, Part D.
2. T. J. Meyer, Acc. Chem. Res., 22 (1989) 163-170.
3. G. J. Kavarnos, N. J. Turro, Chem. Rev., 86 (1986) 401-449.
4. V. Balzani, N. Sabbatini, F. Scandola, Chem. Rev., 86 (1986) 319-337.
5. K. Kalyanasundaram, M. Grätzel, E. Pelizzetti, Coord. Chem. Rev., 69 1986 57-125 and references therein.
6. (a) D. M. Roundhill, H. B. Gray, C.-M. Che, Acc. Chem. Res., 22 1989 55 - 61. (b) J. L. Marshall, A. E. Steigman, H. B. Gray, Excited States and Reactive Intermediates, A. B. P. Lever, (Ed.), ACS Symposium Series 307, American Chemical Society, Washington, DC, 1986, pp 166-176 and references therein.
7. C. L. Hill, D. A. Bouchard, M. Kadkhodayan, M. M. Williamston, J. A. Schmidt, E. F. Hilinski, J. Am. Chem. Soc., 110 (1988) 5471-5479.
8. (a) G. S. Rodman, C. A. Daws, K. R. Mann, Inorg. Chem., 27 1988 3347-3353. (b) G. S. Rodman, K. R. Mann, Inorg. Chem., 24 (1985) 3507-3508.
9. V. M. Miskowski, R. A. Goldbeck, D. S. Kliger, H. B. Gray, Inorg. Chem., 18 (1979) 86-89.
10. J. R.Winkler, D. G. Nocera, T. L. Netzel, J. Am. Chem. Soc., 108 (1986) 4451-4458.
11. R. A. Walton, Isr. J. Chem., 25 (1985) 196-203.
12. (a) F. A. Cotton, K R. Dunbar, L. R. Falvello, M. Tomas, R. A. Walton, J. Am. Chem. Soc., 105 (1983) 4950-4954. (b) F. A. Cotton, M. P. Diebold, C. J. O'Connor, G. L. Powell, J. Am. Chem. Soc., 107 (1985) 7438-7455.
13. D. K. Erwin, G. L. Geoffroy, H. B. Gray, G. S. Hammond, E. I. Solomon, W. C. Trogler, A. A. Zagers, J. Am. Chem. Soc., 99 (1977) 3620-3621.
14. A. Bino, F. A. Cotton, Inorg. Chem., 18 (1979) 3562-3565.
15. I.-J. Chang, D. G. Nocera, J. Am. Chem. Soc., 109 (1987) 4901-4907.

16. M. Anbar, Adv. Chem. Ser., No 50 (1965) 55-81.
17. I.-J. Chang, D. G. Nocera, submitted for publication.
18. C. M. Partigianoni, D. G. Nocera, submitted for publication.
19. M. D. Hopkins, H. B. Gray, Polyhedron, 6 (1987) 705-714.
20. J. M. Canich, F. A. Cotton, K. R. Dunbar, L. R. Falvello, Inorg. Chem., 27 (1988) 804-811.
21. P. E. Fanwick, W. S. Harwood, R. A. Walton, Inorg. Chem., 26 (1987) 242-247.
22. F. A. Cotton, R. A. Walton, Multiple Bonds Between Metal Atoms, Wiley-Interscience, New York, NY, 1982, p 221.